

Experimental validation of numerical model for asymmetric deep drawing of DP780 steel sheet using digital image correlation

X Xue, J Liao, G Vincze and A B Pereira

Centre for Mechanical Technology and Automation, Department of Mechanical Engineering, University of Aveiro, 3810-193, Aveiro, Portugal

Email: xin@ua.pt

Abstract. A validated numerical model for in-plane stress/strain prediction is essential in understanding the deformation behaviour of sheet metal forming process, in particular, asymmetric deep drawing of advanced high strength steel sheet. In this work, the Yld2000-2d anisotropic yield criterion integrated with the initial homogeneous anisotropic hardening model was employed to describe the complex material behaviours of DP780 steel as well as the adoption of Yoshida chord model for elastic modulus degradation. Digital image correlation technique was utilized to measure the in-plane strain and shape deviation of the developed P-channel. The validity of the numerical model was assessed by comparing the predicted strain distribution and twist springback with the measured results. It indicates that the developed numerical model based on the selected constitutive models is acceptable for the deformation analysis, although the predicted discrepancies still exist.

1. Introduction

Advanced high strength steels (AHSS) have become a favourite resource for the weight reduction of automotive industry due to their promising higher strength without compromising ductility. Compared to conventional mild steels, AHSS are prone to strain localization and a subsequent rapid fracture owing to a lower ductility. The challenges for the accurate prediction of strain and elastic-plastic deformation in sheet metal forming process should be highlighted as well as the experimental validation of the developed numerical model.

Nowadays, the use of digital image correlation (DIC) techniques is an efficient tool to collect the experimental forming data and enable the validation of simulation results by direct comparison of the global deformation. In practice, even though the material flow or the overall deformation is usually predicted quite acceptably, the significant discrepancy between the computed and measured strain distributions still exist.

In this work, a new asymmetric experimental benchmark (P-channel) is developed as well as its numerical model in case of deep drawing of DP780 steel sheet. The material constitutive models including the Yoshida chord model [1], the Yld2000-2d anisotropic yield criterion [2] and the homogeneous anisotropic hardening model [3] are adopted to describe the complex elastic-plastic behaviours such as elastic modulus degradation [4], material anisotropy, Bauschinger effect, transient hardening and permanent softening [5]. Special focus will be laid on the analyses of in-plane strain and twist springback for the validation of numerical model using digital image correlation technique.



2. Material characterization and parameter identifications

In this work, DP780 steel sheet with a thickness of 0.8 mm in the as-received state was characterized by using standard uniaxial tension tests along different directions and simple shear tests. The elastic-plastic constitutive models are defined by a yield criterion and a hardening law. The determination of elastic modulus degradation was carried out through uniaxial loading-unloading-loading (ULUL) cycle tension tests and Yoshida-Uemori model, which can be expressed by

$$E_{chord} = E_0 - (E_0 - E_a)[1 - \exp(-\zeta \bar{\epsilon}_p)] \quad (1)$$

where E_a represents the chord modulus obtained for an infinitely large plastic pre-strain $\bar{\epsilon}_p$ and ζ is a material parameter that determines the decrease rate of the unloading elastic modulus E_{chord} .

The anisotropic yield function Yld2000-2d was proposed by Barlat et al. [2], which is given by

$$\phi = |X_1 - X_2|^a + |2X_2 + X_1|^a + |2X_1 + X_2|^a = 2\bar{\sigma}^a \quad (2)$$

The following linear transformation

$$\begin{aligned} \mathbf{X}' &= \mathbf{C}' \cdot \mathbf{s} = \mathbf{C}' \cdot \mathbf{T} \cdot \boldsymbol{\sigma} = \mathbf{L}' \cdot \boldsymbol{\sigma} \\ \mathbf{X}'' &= \mathbf{C}'' \cdot \mathbf{s} = \mathbf{C}'' \cdot \mathbf{T} \cdot \boldsymbol{\sigma} = \mathbf{L}'' \cdot \boldsymbol{\sigma} \end{aligned} \quad (3)$$

written in tensor notation with the stress deviator \mathbf{s} and the stress tensor $\boldsymbol{\sigma}$ allow the introduction of plastic anisotropy. \mathbf{L}' and \mathbf{L}'' provided a total of eight anisotropy coefficients α_k .

The homogeneous anisotropic hardening (HAH) model was proposed to describe the complex mechanical behaviour under stain path changes. It can be briefly presented in the following

$$\Phi(\mathbf{s}) = (\phi_s^q + \phi_f^q)^{\frac{1}{q}} = \left[\phi_s^q + f_1^q |\hat{\mathbf{h}}^s : \mathbf{s} + |\hat{\mathbf{h}}^s : \mathbf{s}|^q + f_2^q |\hat{\mathbf{h}}^s : \mathbf{s} - |\hat{\mathbf{h}}^s : \mathbf{s}|^q \right]^{\frac{1}{q}} = \sigma(\bar{\epsilon}) \quad (4)$$

For the detailed descriptions of this constitutive model, the interested reader can be referred to [3]. Figure 1a shows that the decrease of the elastic modulus for DP780 is 24.0% of its initial value at a 0.09 pre-strain. The comparison of the experimental strain-stress curves and calculated results based on the adopted constitutive models, as shown in Figure 1b, indicates that the hardening model captures well the Bauschinger effect, transient hardening and permanent softening. Table 1 lists all the coefficients of material constitutive models used for simulation.

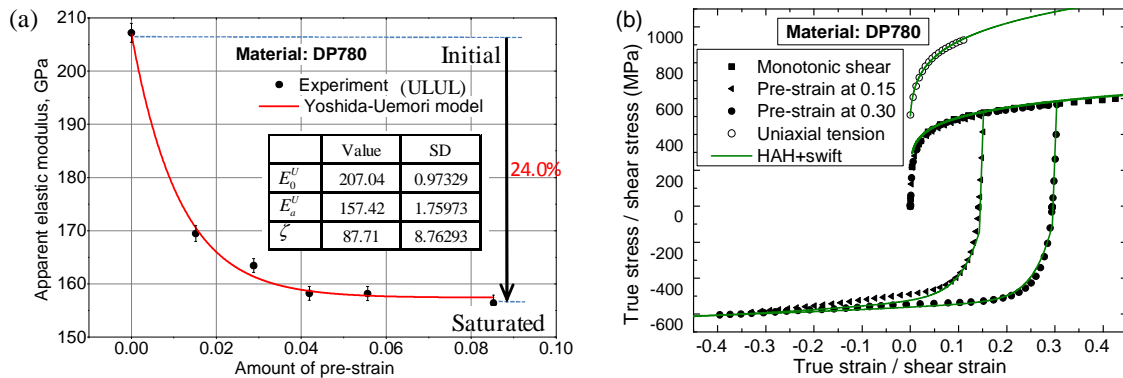


Figure 1. (a) The elastic modulus degradation of DP780 steel (b) comparison of uniaxial and shear stress-strain relations between experiment and calculation results.

Table 1. Material constitutive coefficients of DP780 steel used for simulation.

Yoshida chord model	E_0	E_a	ζ						
	207.04	157.42	87.71						
Yld2000-2d	a	α_1	α_2	α_3	α_4	α_5	α_6	α_7	α_8
	6	0.973	0.879	0.864	0.948	0.999	0.860	0.949	1.030
Initial HAH	q	k	k_1	k_2	k_3	k_4	k_5		
	2	45	50	26.2	0.3	0.9	6.5		
Reference isotropic hardening (Swift law)	ϵ_0	n	K	$\bar{\sigma} = K(\epsilon_0 + \bar{\epsilon}^n)^n$ with $\epsilon_0 = \left(\frac{\sigma_0}{K}\right)^{1/n}$.					
	0.0015	0.151	1298.2						

3. Experimental methodologies

An asymmetric deep drawing benchmark with a variable cross-sectional shape was developed, namely P-channel. It is designed as a U-shaped channel with varied width sweeping along the longitudinal direction, as shown in Figure 2. The section widths are different and kept constant in the both ends but varied through a smooth transition in the middle. Forming this type of channel normally result in considerable deformation behaviours (e.g., twist springback) due to its asymmetric geometry and residual stress distribution. The forming equipment is a SHIMADZU universal tension-compression machine with a maximum capacity 1000 kN. The forming parameters are listed in Table 2. Inverse-install moving die-set was employed to reduce the vibration of the blank holder.

Table 2 Main process parameters of deep drawing.

No.	Parameters	Values
1	Total stroke of deep drawing, mm	40
2	Drawing velocity, mm/min	10
3	Amount of lubricant, g/m ² /side	10-12
4	The quantity of nitrogen gas spring	6
5	Initial/maximum blank holder force, kN	90/144
6	Final press contact pressure, MPa	10
7	Die clearance ratio	1.125

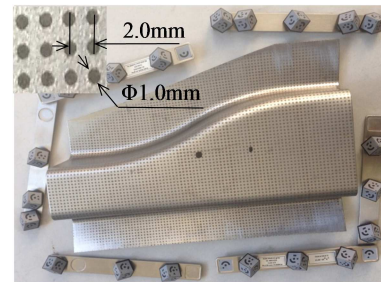


Figure 2. The application of DIC technique

Digital image correlation (DIC) technique was used to assess the deformation of the drawn parts, such as the distribution of in-plane strain, thickness reduction, and geometric shape deviation [6]. Standard grid distance of 2.0 mm and grid diameter of 1.0 mm were marked on the initial blank surface. After the forming, several images were recorded with the ARGUS 5M system, in order to acquire the points positioning from different angles. The 3D reconstruction of the final measuring object was then obtained/computed using the photogrammetric methods.

4. Result and discussion

4.1. In-plane strain

This work aims to validate the selected constitutive models on the prediction of strain and springback for the presented test case. For the selected centre cross section, the discrepancies between the DIC measured stains and the predicted results are shown in Figure 3. It can be seen that the predicted in-plane strain is underestimation at the transition area of the curved side wall compared to the DIC experimental results.

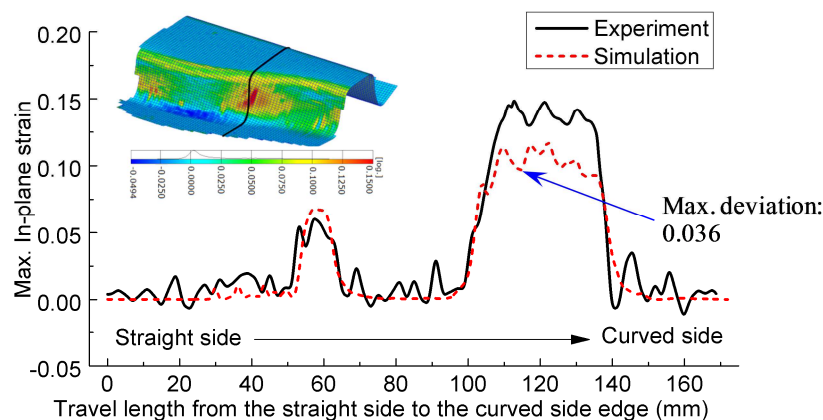


Figure 3. Comparison of the in-plane strain field of the selected cross section by DIC measurement and numerical prediction for DP780 P-channel.

Even though the simulated results for material flow are in reasonable agreement with the experiments, some significant differences exist between the computed and measured strain fields. This might be due to the point pattern of the measured object and the lack of fitting accuracy of the deformed circles because of the severe strain variations. This error deviation of in-plane strain can be up to 0.02. It also might be due to the deviation of the material description implemented into the simulation code [7]. These discrepancies should be reduced or eliminated with the development of advance deformation measurement technology and more comprehensive material constitutive models.

4.2. Preliminary result of twist springback

Figure 4 shows the displacement springback distribution along the Z-direction or 3-direction (U3) and comparison of the measured twist springback and the predicted results. It is observed that the displacement of the flange along the straight side has a significant variation while that along the curved side is almost stable, indicating the occurrence of the twisting. The relative twist angle defined as the rotation angle of the principal axis of inertia for the cross-section before and after springback [6] decreases fast initially in the narrow sections, then it starts slightly fluctuating in the sections located in the transition region, where the width of the cross section varies. After the transition region, it starts decrease again in the wide sections. The evolution of the predicted relative twist springback agrees well with the experiment. Although the predicted discrepancies still exist, the validity of the developed numerical model is acceptable for the deformation analysis.

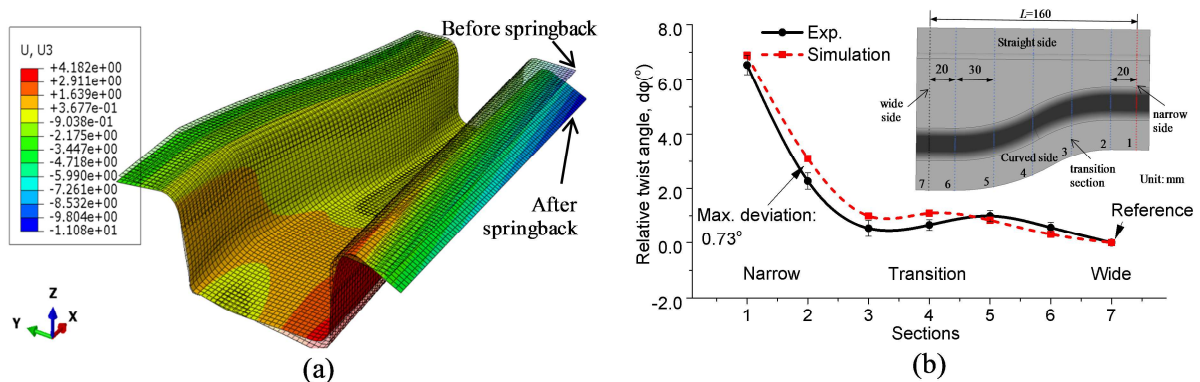


Figure 4. (a) The displacement springback distribution along the Z-direction (b) comparison of the measured relative twist angle of the DP780 P-channel and simulation results.

5. References

- [1] Yoshida F, Uemori T and Fujiwara K 2002 *Int. J. Plast.* **18** 633
- [2] Barlat F, Brem J C, Yoon J W and Chung K 2003 *Int. J. Plast.* **19** 1297
- [3] Barlat F, Gracio J J, Lee M G, Rauch E F and Vincze G 2011 *Int. J. Plast.* **27** 1309
- [4] Cleveland R and Ghosh A 2002 *Int. J. Plast.* **18** 769
- [5] Yoshida F and Uemori T 2003 *Int. J. Mech. Sci.* **45**(10) 1687
- [6] Xue X, Liao J, Vincze G, Sousa J A, Barlat F and Gracio J 2016 *Mater. Des.* **90** 204
- [7] Xue X, Liao J, Vincze G and Barlat F 2015 *Int. J. Mater. Form.* (doi: 10.1007/s12289-015-1275-2)

Acknowledgments

The support from the Portuguese Foundation of Science and Technology (UID/EMS/00481/2013 and PTDC/EMS-TEC/0777/2012) is greatly appreciated. The authors are grateful to Prof. Myoung-Gyu Lee of Korea University for providing user-material subroutine code of the HAH model.